MM Science Journal | www.mmscience.eu
ISSN 1803-1269 (Print) | ISSN 1805-0476 (On-line)
Special Issue | CUTTING TOOLS 2024
1st International Conference on Cutting Tools
November 20-22, 2024, Trnava, Slovakia
DOI: 10.17973/MMSJ.2025_06_2025034

CUTTINGTOOLS2024-00014

THE EFFECT OF TECHNOLOGICAL PARAMETERS ON THE CHANGE IN SURFACE MICROHARDNESS DURING THE EXTERNAL CYLINDRICAL BURNISHING OF X5CRNI18-10 STEEL WORKPIECES

G. Varga[1]*, S. Smolnicki[1]
[1]University of Miskolc, Institute of Manufacturing Science, Miskolc, Hungary
*Corresponding author; e-mail: gyula.varga@uni-miskolc.hu

Abstract
Among the finishing machining operations, burnishing is an economical process with a low environmental impact. In special cases, grinding can be replaced by burnishing, creating the same roughness with a much lower environmental load. The purpose of the study was to determine the effect of the technological parameters of the burnishing process on the surface roughness and hardness. The hardening experiments were performed on X5CrNi18-10 stainless steel specimens. The burnishing parameters used during the experimental examinations were burnishing speed, feed, and burnishing force. The experiments were carried out using the full factorial experimental design method.
After the evaluation of the measured results, it was determined that due to burnishing, from the pre-burnishing value of the Vickers hardness HV: 330-370 increased to HV: 380-490. A special improvement-ratio formula was developed to evaluate the effectiveness of the burnishing process in terms of hardness and roughness.

Keywords:
Sliding friction burnishing, Stainless steel, Surface roughness, Hardness, Surface layer

1 INTRODUCTION

In the context of the ongoing 4th Industrial Revolution, ensuring finer surface quality of manufactured components has become increasingly important [Kovács 2020]. According to researchers, the durability and reliability of machine parts depend on the outcome of the manufacturing process and the surface structures formed [Sztankovics 2023]. The surface structure influences the wear and fatigue strength of the component [Kundrák 2022]. Machined parts often require additional finishing operations, such as grinding. However, this process may require further processing, such as burnishing. During the burnishing process, the surface undergoes plastic deformation, which is performed using ball burnishing or sliding burnishing tools. As a result, the surface roughness decreases, and the surface layer becomes harder [Ferencsik 2023], [Tesfom Kebede 2024]. The burnishing process can also be performed on a universal lathe. Diamond burnishing, a sliding friction-based machining process, is like turning; however, it does not produce chips, and therefore no chip removal is done [Varga 2023].

Numerous studies focus on the development of burnishing technology, with particular attention to the optimization of surface quality, wear resistance, microhardness, and residual stresses. Two main areas can be observed: ball burnishing and diamond burnishing based on sliding friction. The works of Velázquez-Corral, Cagan, Nguyen, Swirad, and Rami dealt with ball burnishing, while Zhang, Sachin, He, Maximov, Mirjalili, John, Sarhan, Grzesik, and Bouzid focused on sliding friction-based diamond burnishing.

Velázquez-Corral et al. [Velázquez-Corral 2024] investigated the effect of ultrasonic assistance during ball burnishing on Ti6Al4V alloy. As a result of a 170 N burnishing force, 3 passes, and 40 kHz vibration, surface roughness decreased from 1.50 to 0.45 μm, while the friction force essentially remained unchanged.

Cagan et al. [Cagan 2022] examined minimum quantity lubrication (MQL)-assisted burnishing on WE43 magnesium alloy. Using a Taguchi design, they identified optimal parameters that significantly improved microhardness and surface roughness; the force parameter proved to be the most influential.

Nguyen T. and Le C. [Nguyen 2021] focused on optimizing the 6061 aluminum CATB (compressed air turning-burnishing) process. Through Kriging modeling, they identified parameters (e.g., 196.3 N burnishing force) that resulted in a 65.38% reduction in roughness and a 30% increase in hardness, while also reducing energy consumption.

Swirad [Swirad 2019] concentrated on the 3D surface texture of hydrostatic burnishing on X38CrMoV5-1 steel. Using second-order polynomial modeling, the positive effect of the technology on surface geometry parameters was demonstrated.

Rami A. and colleagues [Rami 2018] applied a combined turning-burnishing process on AISI 4140 steel. The process increased productivity and improved surface integrity, with parameter optimization performed using the Taguchi method.

Zhang and colleagues [Zhang 2020] examined the effect of the initial surface roughness produced by turning on the effectiveness of burnishing during the refurbishment of hydraulic support columns of mining equipment. Two types of turning inserts (traditional and wiper) were used, and their impact on burnishing-induced roughness and residual stress development was compared. Traditional inserts showed a positive correlation, while wiper inserts showed a negative correlation with improvements. Additionally, initial roughness significantly influenced the residual stress level after burnishing, which is crucial for the lifespan of structural components.

Sachin and colleagues [Sachin 2019] focused on optimizing the diamond burnishing process for 17-4 PH stainless steel. A new type of diamond tool was used, operating in an MQL environment, and the effects of process parameters such as speed, feed rate, and force on surface characteristics were investigated. Optimization was carried out using a genetic algorithm. The results demonstrated the effectiveness of diamond burnishing, achieving significant improvements in surface roughness and hardness.

He D. and colleagues [He 2017] investigated the mechanism of residual stresses formed during the burnishing process. They found that the so-called interference effect—where previous burnishing points affect subsequent ones—played a significant role. By reducing the feed rate, this effect increased. The findings may help ensure a longer fatigue life for critical components, such as turbine blades.

Maximov J.T. and colleagues [Maximov 2016] examined the sliding friction ball burnishing of D16T aircraft aluminum alloy. They analyzed how process parameters such as burnishing pass number and lubrication affect surface roughness, microhardness, and residual stress. FEM simulations were used to determine the impact of burnishing force and tool radius on the stress profile. The optimized parameters significantly improved the mechanical properties of the material.

Mirjalili S. and colleagues [Mirjalili 2014] applied the grey wolf optimization algorithm to optimize the burnishing process. This nature-inspired method is effective for mapping nonlinear, complex search spaces, making it highly applicable to burnishing parameter optimization. Their results indicated that the algorithm effectively calculates optimal technological parameters, even for complex surface responses.

John M.R. and colleagues [John 2014] investigated the effectiveness of burnishing on materials with low ductility, such as brass, EN24, AISI 1020, and 6061 aluminum. High-speed burnishing with low force was used, and surface roughness, micro-Vickers hardness, and cylindricity deviation were analyzed. The results showed that burnishing significantly improved surface properties for all materials.

Sarhan A.A. and El-Tayeb N.S. [Sarhan 2013] modeled the surface roughness after burnishing of C3605 brass using a fuzzy rule-based system. The predictive model forecasted Ra values with 95.4% accuracy based on various parameters, including burnishing speed, feed rate, and depth of cut. This method can assist in faster and more reliable burnishing parameter design.

Grzesik W. and Żak K. [Grzesik 2012] investigated how surface quality produced by hard turning could be further improved by burnishing and superfinishing. In experiments conducted on 41Cr4 steel, various insert types (including Wiper) were analyzed. Burnishing significantly improved both 2D and 3D roughness parameters, and the process complemented hard turning effectively.

Bouzid W. and colleagues [Bouzid 2024] examined the burnishing of AISI 1042 steel surfaces after prior turning and/or grinding. They found that burnishing, especially with low feed rates, provided excellent surface quality, which could even replace grinding. Additionally, compressive residual stresses formed, improving the fatigue resistance of the components.

The aim of the study presented in this paper is to determine the effect of technological parameters applied during the burnishing of X5CrNi18-10 material specimens on the 3D surface roughness parameters. Empirical functions were created when evaluating the experiments implemented using the full factorial design of experiments. A special dimensionless improvement ratio factor helps to better evaluate the efficiency of the hardening process in relation to roughness.

2 APPLICATION OF SLIDING FRICTION DIAMOND BURNISHING ON EXTERNAL CYLINDRICAL SURFACES

Burnishing is a cold plastic deformation process that is also used for the finishing of external cylindrical surfaces. The process offers numerous advantages, including reduced surface roughness, increased microhardness, the induction of compressive residual stresses, improved dimensional accuracy, and environmental friendliness, as it does not require large amounts of coolant or lubricant [Maximov 2015].

Figure 1 [Varga 2023] illustrates the mechanism of diamond burnishing, in which a spherical-tip diamond tool, moved with specific parameters and force, makes contact with the surface of a rotating workpiece. The tool moves in a straight, uniform motion parallel to the workpiece's axis of rotation.

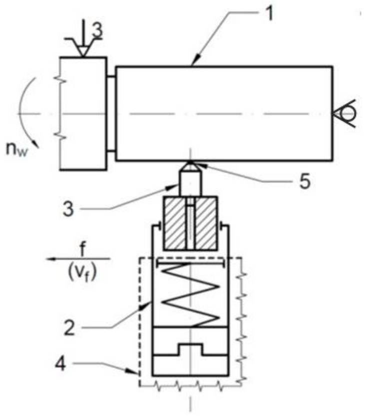

Fig. 1: Kinematic sketch of diamond burnishing.

(1 - workpiece, 2 - burnishing tool, 3 - burnishing insert, 4 - tool holder, 5 - diamond tip), f – feed, v_f – feed rate, n_w – revolution number of the workpiece [Varga 2023]

3 EXPERIMENTAL CONDITIONS

3.1 Material, specimen

Austenitic chromium-nickel steel type X5CrNi18-10 has outstanding corrosion resistance, cold formability and weldability, making it the most widely used and widespread type of stainless steel. It is resistant to weak acids, water and humidity. X5CrNi18-10 type stainless steel is regularly used in various industrial sectors. This stainless steel is also regularly used in automotive manufacturing (vehicle manufacturing). In machine and device manufacturing, machine and pump parts are made from this material. This material is widely used due to its excellent intergranular corrosion resistance, which can be further increased by cold forming processes, such as diamond burnishing. That is why this material was the subject of our investigation. Its chemical composition is given in Table 1 [metalcore 2020], and its mechanical properties are given in Table 2 [metalcore 2020].

The physical properties of X5CrNi18-10 stainless steel at 20°C were as follows [metalcore 2020]: Density 7.9 g/cm³, Specific heat capacity 500 J/kg K, Thermal conductivity 15 W/m K, Electrical resistivity 0.73 Ωmm²/m.

Tab. 1: Chemical composition (wt.%) of austenitic chromium-nickel stainless steel X5CrNi18-10 [metalcore 2020]

C %	Si %	Mn %	P %
≤ 0.07	≤ 1.00	≤ 2.00	≤ 0.045
S %	Cr %	Ni %	N %
≤ 0.015	17.5-19.5	8.00-10.5	≤ 0.11

Tab. 2: Mechanical properties of austenitic chromium-nickel stainless steel X5CrNi18-10 at 20 °C [metalcore 2020]

Hardness HB 30	0.2% Yield strength, Rp	Tensile strength, Rm	Elongat-ion A5	Modulus of elasticity
HB	N/mm²	N/mm²	%	kN/mm²
≤ 215	≥ 190	500-700	≥ 45/35	200

The geometric dimensions of the specimen used for the burnishing experiments were: 5 adjacent cylindrical surfaces with a diameter of Ø49.48 mm and a length of 26 mm. The surface roughness data of the specimen before burnishing can be found in the tables below.

3.2 Research methodology

For the present series of experiments, the effects of three factors were examined, each factor was varied at 2-2 levels according to the full factorial experimental design (Fridrik 1987). The advantage of the method is that an empirical functional relationship can be written between the input (independent) parameters and the output (dependent) variable. The independent variables are called factors. The different set values of the factors are called levels.

The burnishing experiments were performed on a renovated, sufficiently rigid EU-400/01 type SZIM lathe located at the Institute of Manufacturing Science of the University of Miskolc. The material of the burnishing tool was PCD and its radius R=3.5 mm. The SAE 15W-40 type lubricating oil was manually dosed in an amount of $Q_o = 5\times10^{-6}\pm1\times10^{-6}$ m³. The experimental design matrix for the changes in burnishing parameters is given in Table 3 for burnishing forces F_1-F_4. Table 4 concerns forces F_2-F_4, while Table 5 concerns to forces F_3-F_4.

Table 3. Burnishing parameter variations for F_1-F_4

	Burnishing parameters		
	v [m/min]	f [mm/rev]	F_1-F_4 [N]
1	41.17	0.0125	10
2	58.26	0.0125	10
3	41.17	0.0500	10
4	58.26	0.0500	10
5	41.17	0.0125	40
6	58.26	0.0125	40
7	41.17	0.0500	40
8	58.26	0.0500	40

Table 4. Burnishing parameter variations F_2-F_4

	Burnishing parameters		
	v [m/min]	f [mm/rev]	F_2-F_4 [N]
1	41.17	0.0125	20
2	58.26	0.0125	20
3	41.17	0.0500	20
4	58.26	0.0500	20
5	41.17	0.0125	40
6	58.26	0.0125	40
7	41.17	0.0500	40
8	58.26	0.0500	40

Table 5. Burnishing parameter variations F_3-F_4

	Burnishing parameters		
	v [m/min]	f [mm/rev]	F_3-F_4 [N]
1	41.17	0.0125	30
2	58.26	0.0125	30
3	41.17	0.0500	30
4	58.26	0.0500	30
5	41.17	0.0125	40
6	58.26	0.0125	40
7	41.17	0.0500	40
8	58.26	0.0500	40

The surface microhardness of the specimens was measured at three points 120° apart using a Wilson Instruments Tukon 2100B Vickers hardness tester located at the Institute of Metallurgical Forming and Nanotechnology at the University of Miskolc. During the test, dimensionless ratios were created using formulas (1) and (2):

$$\rho_{HV} = \frac{HV_{02,v}}{HV_{02,e}} \tag{1}$$

$$IHV_{02}\ \% = (\rho_{HV} - 1) \cdot 100\ \% \tag{2}$$

where:

ρ_{HV} - Dimensionless hardness improvement ratio

HV_{02v} / HV_{02e} - Hardness after/before burnishing, HV

IHV_{02} - Percentage change in the improvement ratio, %

The introduction and use of the dimensionless improvement ratio was justified by material inhomogeneity. Before burnishing, the surfaces of the test piece may have different hardnesses. This dimensionless ratio can take into account the effect of the increase in the actual hardness of burnishing process. The surface microhardness of the specimens was measured at three points 120° apart using a Wilson Instruments Tukon 2100B Vickers hardness tester located at the Institute of Metallurgical Forming and Nanotechnology at the University of Miskolc. During the test, dimensionless ratios were created using formulas (1) and (2):

4 MEASUREMENT RESULTS OF SURFACE MICROHARDNESS

The surface microhardness measurement results and the calculated improvement ratios for the F_1-F_4 burnishing force variants are contained in Table 6, for the F_2-F_4 burnishing force variant in Table 7, and for the F_3-F_4 burnishing force variant in Table 8.

Table 6. The microhardness improvement ratio ($IHV_{1\text{-}4}$) when applying the burnishing forces F_1-F_4

	Burnishing parameters			Before burnish	After burnish	$IHV_{1\text{-}4}$
	v [m/min]	f [mm/rev]	F [N]	HV_b	HV_a	IHV %
1	41.17	0.0125	10	346.33	429.67	24.064
2	58.26	0.0125	10	324.00	419.67	29.528
3	41.17	0.0500	10	332.33	406.67	22.369
4	58.26	0.0500	10	338.00	388.00	14.793
5	41.17	0.0125	40	344.33	470.00	36.497
6	58.26	0.0125	40	347.33	488.00	40.500
7	41.17	0.0500	40	335.00	455.67	36.021
8	58.26	0.0500	40	365.00	461.00	26.301

Table 7. The microhardness improvement ratio ($IHV_{2\text{-}4}$) when applying the burnishing forces F_2-F_4

	Burnishing parameters			Before burnish	After burnish	$IHV_{2\text{-}4}$
	v [m/min]	f [mm/rev]	F [N]	HV_b	HV_a	IHV %
1	41.17	0.0125	20	349.33	429.00	22.807
2	58.26	0.0125	20	338.00	418.33	23.766
3	41.17	0.0500	20	350.00	422.67	20.763
4	58.26	0.0500	20	325.67	428.67	31.627
5	41.17	0.0125	40	344.33	470.00	36.497
6	58.26	0.0125	40	347.33	488.00	40.500
7	41.17	0.0500	40	335.00	455.67	36.021
8	58.26	0.0500	40	365.00	461.00	26.301

Table 8. The microhardness improvement ratio ($IHV_{3\text{-}4}$) when applying the burnishing forces F_3-F_4

	Burnishing parameters			Before burnish	After burnish	$IHV_{3\text{-}4}$
	v [m/min]	f [mm/rev]	F [N]	HV_b	HV_a	IHV %
1	41.17	0.0125	30	359.67	440.67	22.521
2	58.26	0.0125	30	367.33	468.00	27.406
3	41.17	0.0500	30	356.33	439.33	23.293
4	58.26	0.0500	30	365.00	468.67	28.403
5	41.17	0.0125	40	344.33	470.00	36.497
6	58.26	0.0125	40	347.33	488.00	40.500
7	41.17	0.0500	40	335.00	455.67	36.021
8	58.26	0.0500	40	365.00	461.00	26.301

An illustration of the empirical formulas (3-5) determined with the MathCAD 15 program is shown in Figures 3-5.

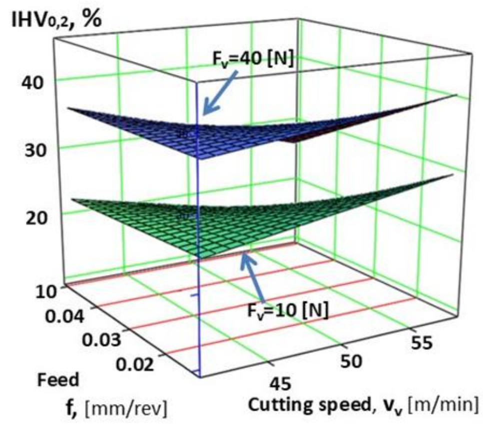

Fig. 3. Change in microhardness improvement ratio ($IHV_{1\text{-}4}$) when applying the burnishing forces F_1-F_4

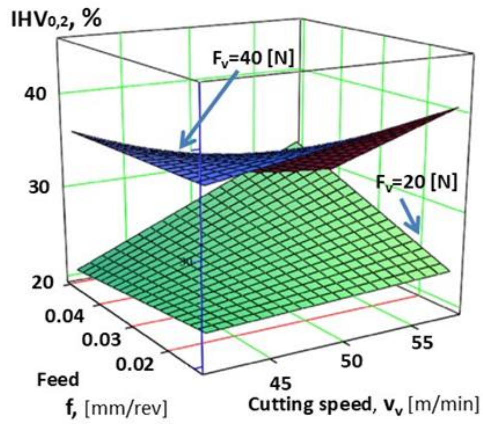

Fig. 4. Change in microhardness improvement ratio ($IHV_{2\text{-}4}$) when applying the burnishing forces F_2-F_4

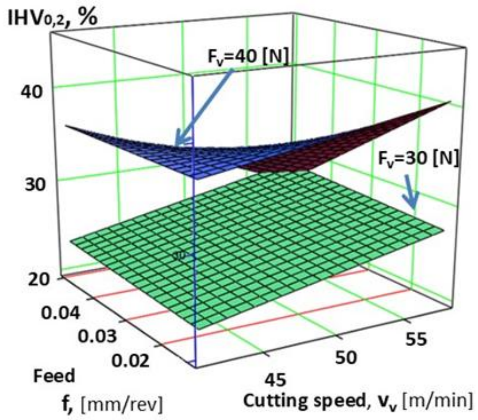

Fig. 5. Change in microhardness improvement ratio ($IHV_{3\text{-}4}$) when applying the burnishing forces F_3-F_4

$$IHV_{10-40} = -4{,}0064 + 0{,}598v + 767{,}16f + 0{,}5F - 19{,}993vf - 0{,}0024vF + 2{,}541fF - 0{,}035vfF \quad (3)$$

$$IHV_{20-40} = 42{,}2658 - 0{,}776v - 2250f + 0{,}657F + 52{,}318vf - 0{,}032vF + 77{,}979fF - 1{,}843vfF \quad (4)$$

$$IHV_{30-40} = -5{,}2597 - 0{,}38v - 2582f + 0{,}532F + 65{,}63vf + 0{,}022vF + 86{,}261fF - 2{,}176vfF \quad (5)$$

5 DISCUSSION

During the evaluation, the microhardness improvement ratios for each burnishing force applied were determined in Tables 6-8. The best hardness improvement values for different burnishing forces are included in Table 8.

Table 8. The microhardness improvement ratio (IHV) when applying different burnishing forces

	Burnishing parameters			Before burnish	After burnish	IHV
	v [m/min]	f [mm/rev]	F [N]	HV_b	HV_a	IHV %
	58.26	0.0125	**10**	324.00	419.67	29.528
	58.26	0.0500	**20**	325.67	428.67	31.627
	58.26	0.0500	**30**	365.00	468.67	28.403
	58.26	0.0125	**40**	347.33	488.00	40.500

Table 8 clearly shows that the largest hardness improvement ratios are achieved at higher (v_2=58.26 m/min) burnishing speeds. There is no linearity between the increase in the burnishing force and the values of the hardness improvement ratio. The smallest improvement ratio occurred when the burnishing force F=30 N was applied, while the largest value could be get when the applied force F=40 N was.

Furthermore, we examined which technological parameter changes result in hardness improvements and their magnitude. This is contained in Table 9.

Table 9. The microhardness improvement ratio (IHV) when applying different burnishing forces

		Improvement of HV		Difference
Applied parameters	**F_1**	v_2, f_2	v_2, f_1	ΔIHV
		29.528	22.369	7.159
Applied parameters	**F_2**	v_1, f_2	v_2, f_2	
		31.627	20.763	10.864
Applied parameters	**F_3**	v_1, f_2	v_2, f_2	
		28.403	23.293	5.110
Applied parameters	**F_4**	v_2, f_2	v_2, f_1	
		40.50	26.301	14.199

6 CONCLUSIONS, SUMMARY

The study presents the results of experimental examinations on sliding friction diamond burnishing of X5CRNI18-10 stainless steel. The technological parameters examined were burnishing speed, feed rate and burnishing force. The aim of the experiment was to determine which technological parameters result in the highest hardness improvement factors. The full factorial experimental design method was used for the tests. During the evaluation of the results, a dimensionless ratio was formed to visually express the degree of hardness improvement. Empirical formulas were determined for the burnishing force pairs F_1-F_4, F_2-F_4 and F_3-F_4, the content of which was also presented in the form of axonometric 3D diagrams. It was clearly established that the highest hardness improvement ratio was experienced at the higher burnishing speed (v_2=58.26 m/min) for all four applied burnishing forces. However, the situation is not so clear regarding the burnishing feed. In the case of two burnishing forces (F_2=20 N and F_3=30 N), the smaller burnishing feed (f_1=0.0125 mm/rev) resulted in the more favorable hardness improvement factor, while in the case of the other two burnishing forces (F_1=10 N and F_4=40 N) the larger feed (f_2=0.05 mm/rev). Overall, the parameter combination v_2=58.26 m/min, f_2=0.05 mm/rev and F_4=40 N resulted in the largest hardness improvement (IHV_4=40.5 %).

7 REFERENCES

[Kovács 2020] Kovács, Gy. Combination of Lean value-oriented conception and facility layout design for even more significant efficiency improvement and cost reduction. Int. J. of Product. Research, 2020, Vol. 58, No. 10, pp.: 2916–2936.

[Sztankovics 2023] I. Sztankovics, I.: Preliminary Study on the Function-Defining 3D Surface Roughness Parameters in Tangential Turning. International Journal of Integrated Engineering, 2023, Vol. 15, No. 7, pp. 72–81.

[Kundrák 2022] Kundrák, J.; Felhő, Cs.; Nagy, A.: Analysis and Prediction of Roughness of Face Milled Surfaces using CAD Model, Manufacturing Technology, 2022, Vol. 22, No. 5, pp. 558-572.

[Tesfom Kebede 2024] Tesfom Kebede, F.; Felho, C., Examining the impact of slide burnishing parameters on the 3D surface features of medium carbon steel, Journal of Production Engineering, 2024, Vol. 27, No. 1, pp. 30-35,

[Ferencsik 2023] Ferencsik, V.: Analytical analysis of the theoretical surface roughness in the case of burnishing of cylindrical workpiece, Cutting and Tool in Technological Systems, 2023, Vol. 99, pp. 101-109.

[Varga 2023] Varga, G.; Smolnicki, S.; Babič, M.; Caesarendra, W.: Energy Efficiency Analysis When Grinding and Diamond Burnishing of Components, In: Gençyılmaz, M. Güneş; Durakbasa, Numan M. (editors) Towards Industry 5.0: Selected Papers from ISPR2022, Cham, Switzerland: Springer International Publishing, 2023, pp. 378-396.

[Velázquez-Corral 2024] Velázquez-Corral E., et al.: Wear resistance and friction analysis of Ti6Al4V cylindrical ball-burnished specimens with and without vibration assistance, International Journal of Advanced Manufacturing Technology, 2024, Vol. 131, pp.: 551–562

[Cagan 2022] Cagan S.C., Tasci U., Pruncu C.I., Bostan B.: Investigation of the effects of eco-friendly MQL system to improve the mechanical performance of WE43 magnesium alloys by the burnishing process, Journal of the Brazilian Society of Mechanical Sciences and Engineering, 2022, Vol. 45, No. 1

[Nguyen 2021] Nguyen T., Le C.: Optimization of internal burnishing operation for energy efficiency, machined quality, and noise emission, The International Journal of Advanced Manufacturing Technology, 2021, Vol. 114, pp.: 2115–2139

[Zhang 2020] Zhang P., et al.: Effect of turning-induced initial roughness level on surface roughness and residual stress improvements in subsequent burnishing, Archives of Civil and Mechanical Engineering, 2020, Vol. 20, No. 80

[Swirad 2019] Swirad S.: Surface Texture Analysis after Hydrostatic Burnishing on X38CrMoV5-1 Steel, Chinese Journal of Mechanical Engineering (English Edition), 2019, Vol. 32, No. 91

[Sachin 2019] Sachin B., Narendranath S., Chakradhar D.: Journal of the Brazilian Society of Mechanical Sciences and Engineering, 2019, Vol. 41, No. 5.

[Rami 2018] Rami A., Gharbi F., Sghaier S., Hamdi H.: Some insights on Combined Turning-Burnishing (CoTuB) process on workpiece surface integrity, International Journal of Precision Engineering and Manufacturing, 2018, Vol. 19, No. 1, pp.: 67-78

[He 2017] He D., et al.: Investigation of interference effects on the burnishing process, International Journal of Advanced Manufacturing Technology, 2017, Vol. 95, No 1-4, pp. 1-10

[Maximov 2016] Maximov J.T., et al.: Influence of the process parameters on the surface roughness, micro-hardness, and residual stresses in slide burnishing of high-strength aluminum alloys, Journal of the Brazilian Society of Mechanical Sciences and Engineering, 2016, Vol. 39, No. 8, pp.: 3067-3078

[Mirjalili 2014] Mirjalili S., Mirjalili S.M., Lewis A.: Grey Wolf Optimizer, Advances in Engineering Software, 2014, Vol. 69, pp. 46-61

[John 2014] John M.R., Suresh P., Raguraman D., Vinayagam B.K.: Surface Characteristics of Low Plasticity Burnishing for Different Materials Using Lathe, Arabian Journal for Science and Engineering, 2014, Vol. 39, No. 4, pp. 3209-3216

[Sarhan 2013] Sarhan A.A., El-Tayeb N.S.: Investigating the surface quality of the burnished brass C3605—fuzzy rule-based approach, International Journal of Advanced Manufacturing Technology, 2013, Vol. 71, No. 5-8, pp.: 1143-1150.

[Grzesik 2012] Grzesik W., Żak K.: Modification of surface finish produced by hard turning using superfinishing and burnishing operations, Journal of Materials Processing Technology, 2012, Vol. 212, pp.. 315–322

[Bouzid 2004] Bouzid W., Tsoumarev O., Sa K.: An investigation of surface roughness of burnished AISI 1042 steel, International Journal of Advanced Manufacturing Technology, 2004, Vol. 24, pp.: 120-125.

[Maximov 2015] Maximov, J.T., Anchev, A.P. and Duncheva G.V.: Modeling of the friction in the tool workpiece system in diamond burnishing process, Coupled Systems Mechanics, 2015, Vol. 4, No. 4 pp.: 279-295,

[metalcore 2020] http://www.metalcor.de/en/datenblatt/5/ (2020.05.17)

Fridrik, L.: Selected chapters on the topic of designing engineering technology experiments. Tankönyvkiadó, Budapest, 1993, (In Hungarian)